SMAR 2015 – Third Conference on Smart Monitoring,
Assessment and Rehabilitation of Civil Structures

SMAR 2015

# FRP/stirrups interaction for mechanically fastened FRP strengthened beams in shear

Usama Ebead[1]

[1] Qatar University, Doha, Qatar

ABSTRACT: This research aims at creating precise finite element models for FRP shear strengthened concrete beams. The models will be developed to assess the shear behaviour of beams strengthened using the externally bonded (EB), mechanically fastened (MF), and hybrid EB / MF fibre-reinforced polymer (FRP) systems. The interfacial behaviour between the hybrid EB/MF-FRP and the concrete will be accounted for, here, using specially developed interface elements. A user-defined subroutine for the microplane constitutive law for the concrete material will be incorporated in the model. A special emphasis will be placed on the interaction between the internal reinforcement (stirrups) and the external FRP strips. Results will be presented in terms of the ultimate load carrying capacities, interfacial stress/slip distributions, and the interaction of FRP/stirrups. Numerical results are validated against available experimental results and show reasonable agreement.

## 1 INTRODUCTION

Recently, researchers have shown an increased interest in developing numerical tools based on the finite element analysis for determining the interfacial behaviour between the FRP systems and the concrete substrate in attempts to better understand such a complex behaviour when these systems are used for strengthening reinforced concrete (RC) beams (Neale, Ebead et al. 2006, Abdel Baky, Ebead et al. 2007, Kotynia, Abdel Baky et al. 2008, Ebead and Saeed 2013) and slabs (Ebead and Marzouk 2005, Elsayed, Ebead et al. 2007, Ebead and Saeed 2010). This is due to the fact that the interfacial behaviour is difficult to be accurately determined using physical experiments. Externally bonded (EB) FRP strengthening technique has proven great success when used for shear capacity enhancement of RC beams. However, a major problem with such a strengthening technique is debonding. End anchorage of the FRP plates or strips is a common remedy for mitigating debonding leading to an increase in the load capacity of shear strengthened RC.

A strengthening technique that is characterized by its ductile behaviour and uses mechanically fastened (MF) FRP strips with closely spaced nails/fasteners has been introduced for concrete structures (Lamanna, Bank et al. 2004, Lamanna, Bank et al. 2004, Bank and Arora 2007). This technique utilizes simple tools to attach pultruded FRP strips to the concrete. In the work done by Lamanna and co-workers a powder-actuated type of fasteners was used to attach the FRP strips to the concrete (Lamanna, Bank et al. 2004, Lamanna, Bank et al. 2004). In other contributions, small diameter threaded fasteners were utilized for the flexural (Ebead 2011) and shear (Ebead and Saeed 2013) strengthening of RC beams, for the strengthening of RC two-way slabs with and without cut-outs (Elsayed, Ebead et al. 2009), and for the direct shear application (Elsayed, Ebead et al. 2009).

The hybrid EB/MF-FRP system is in essence a combination of the externally bonded and the mechanically fastened systems. The advantage of the relatively closely spaced fasteners is the fact that these fasteners act as anchorages; therefore mitigate debonding. The experimental results indicated that the hybrid EB/MF strengthened specimens consistently showed better strength performance than those strengthened using the MF strengthened specimens and better deformational and ductility performances than those strengthened using the EB system for both the shear (Ebead and Saeed 2013) and flexural (Ebead 2011) applications. Numerical finite element models have been also created and verified for the flexural application of reinforced concrete beams strengthened using the three aforementioned strengthening systems (Ebead and Saeed 2013).

Finite element packages have been employed to model the structural behaviour of both passive as well as externally bonded FRP shear strengthened concrete beams where the bond between the FRP composites and the beams is accounted for (Godat, Neale et al. 2007, Chen, Chen et al. 2012, Godat, Labossiere et al. 2012, Godat, Labossière et al. 2012).

In this study, special interface elements to represent the interfacial behaviour between the concrete and the FRP composites (at the bonded and mechanically fastened locations) are implemented in the models. Results are presented here in terms of the ultimate load carrying capacities, load–deflection relationships, FRP strains and interfacial stress distributions. Experimental results of RC beams strengthened using the EB-, MF- or hybrid EB/MF-FRP strengthening systems (Ebead and Saeed 2013) are used to validate the models in terms of the ultimate load capacities and deformational characteristics. Details of the experimental work can be found in the work completed by the authors (Ebead and Saeed 2013). Configuration of the experimentally tested strengthened beams is listed in Table 1. The designation of each specimen is made so that ‘‘R’’ is for ‘‘reference specimen’’. ‘‘M’’ is for ‘‘mechanically fastened’’, ‘‘B’’ is for ‘‘externally bonded’’ and therefore ‘‘BM’’ is for the ‘‘hybrid externally bonded-mechanically fastened’’. Numerals 6 and 8 refer to the use of 6 or 8 strips, respectively, on each side of the beam web. Letters N and W refer to the use of narrow and wide strips, respectively. The specimens with vertical and inclined strips use the letters ‘‘V’’ and ‘‘I’’, respectively in their designations. Letter ‘‘S’’ is for specimens with stirrups within the critical shear span.

## 2 FINITE ELEMENT MODELLING

The numerical analysis is carried out using the finite element software package ADINA (Bathe 2005). The concrete compressive and tensile strengths for each specimen are obtained from the original experimental work (Ebead and Saeed 2013) to be used in the material model definition. Description of the material modelling, finite elements used and the simulated boundary conditions are presented hereafter.

### *2.1 Material Modelling*

The M4 version of the microplane model is used here to define the concrete constitutive behaviour (Bažant, Caner et al. 2000, Caner and Bažant 2000). The concrete characteristics obtained experimentally (Ebead and Saeed 2013) have been used in the model. The longitudinal and transverse steel reinforcement bars are modelled as bilinear elastic-plastic materials, with the tangent modulus in the strain-hardening zone taken to be 1/100 of the elastic modulus. Properties of the steel reinforcement and the FRP strips are based on the original experimental work. The yield stresses for the steel reinforcement bars as given in the original reference are 522 MPa, 516 MPa , and 410 MPa for the bars of diameters of 14 mm (for the main reinforcement), 8 mm (for the top reinforcement), and 6 mm (for the transverse

reinforcement), respectively. The average FRP modulus of elasticity, $E_{FRP}$, and tensile strength, $f_{FRP}$, have been taken as 72.02 GPa and 1003.4 MPa, respectively. The FRP strip widths are 102 mm for the wide strips and 51 mm for the narrow strips and the thickness is 3.2 mm. A linear elastic orthotropic constitutive relation was assumed for the FRP composites. The elastic modulus in the direction perpendicular to the fibres was assumed to be one tenth of that in the direction of the fibres. For the FRP/concrete interface, two different interfacial models are employed in this work. The first model is the interfacial shear stress–slip model for the EB-FRP system. The second model is applied at the locations of fasteners in the MF-FRP and hybrid EB/MF-FRP system and is referred to as the bearing stress–slip model. Details of the interface models for both the externally bonded and mechanically fastened locations can be found in (Elsayed, Ebead et al. 2009). Figure 1a and 1b show the interfacial shear stress-slip relationship adopted for EB-FRP locations of the strengthened specimens and the interfacial bearing stress-slip slip relationship adopted for MF-FRP counterparts.

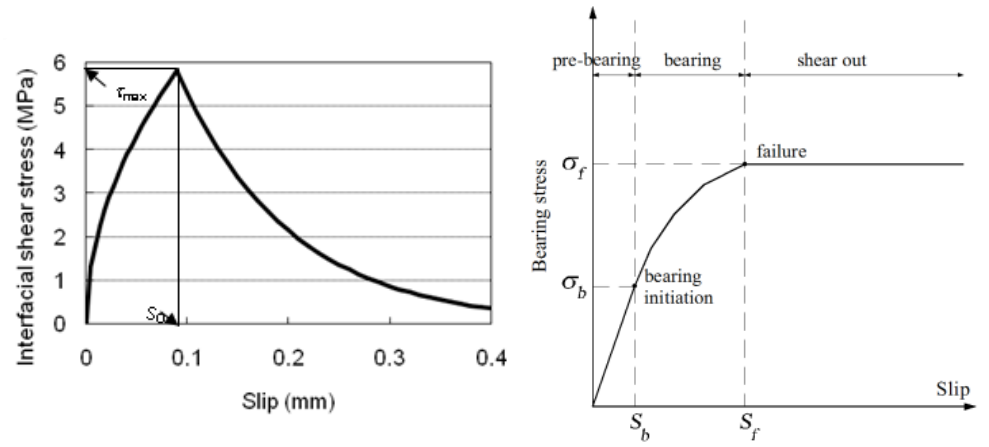


a) Bond-slip model b) Bearing- slip model

Figure 1. Interfacial stress-slip relationship adopted for (a) the EB FRP strengthened specimens and (b) the mechanically fastened FRP strengthened specimens.

### *2.2 Geometrical Modelling, Loading and Boundary Conditions*

For the shear application, building a 3D model is essential. Therefore, investigating the behaviour of shear strengthened beams is in general more challenging and complex as far as the models created are concerned as compared to those of the flexural strengthened specimens (Ebead and Saeed 2014).Three-dimensional finite element model used in this investigation for a vertical FRP strengthened specimen is depicted in Figure 2. Three-dimensional 27-node brick elements with three degrees of freedom per node are employed to define the concrete beams. Only one half of a beam specimen is modelled due to the geometrical symmetry with respect to a longitudinal place intersection mid-width of the beam, as per Figure 2. The steel reinforcement bars in the longitudinal and transverse directions are represented using 3-node truss elements. Each element has two translational degrees of freedom at each node. The nodes of these truss elements have full constraint compatibility with the in-common nodes of the 3-D concrete elements, i.e., full bond between the concrete and the steel reinforcement is enforced. The different FRP configurations listed in Table 1 are modelled. Nine-node thin shell elements with three degrees of freedom at each node are used for the FRP strips. The orthotropic nature of the

FRP composites is considered in the constitutive relation of the material. Truss elements aligned in the direction of the FRP longitudinal fibres are employed to represent the FRP/concrete interface as shown in Figure 2. Each element has two nodes, each with two degrees of freedom. The internal deformation of an element represents the interfacial slip. The area of an interface element for the bonded locations is evaluated as the area that surrounds the element it represents. For the mechanically fastened locations, the area of the interface element is represented by the contact bearing area between the fastener and the FRP. This area is equal to the FRP strip thickness multiplied by the fastener diameter. In Figure 2, the constraint equations are enforced in the FRP length direction between the first interface node NI(i) and the concrete node NC(i) and between the second interface node NI(i+1) and the FRP node NF(i).

### *2.3 Loading and boundary conditions*

Displacement control loading is used in the model to capture the entire load–deflection plateau. The location of the applied displacement is as shown in Figure 2 for a sample finite element model of a strengthened specimen. The load that causes each displacement is evaluated as the summation of the vertical reactions associated with each load step at the support locations. Contact surface is used at the support location to avoid stress concentration and to simulate the actual supports in the experimental work.

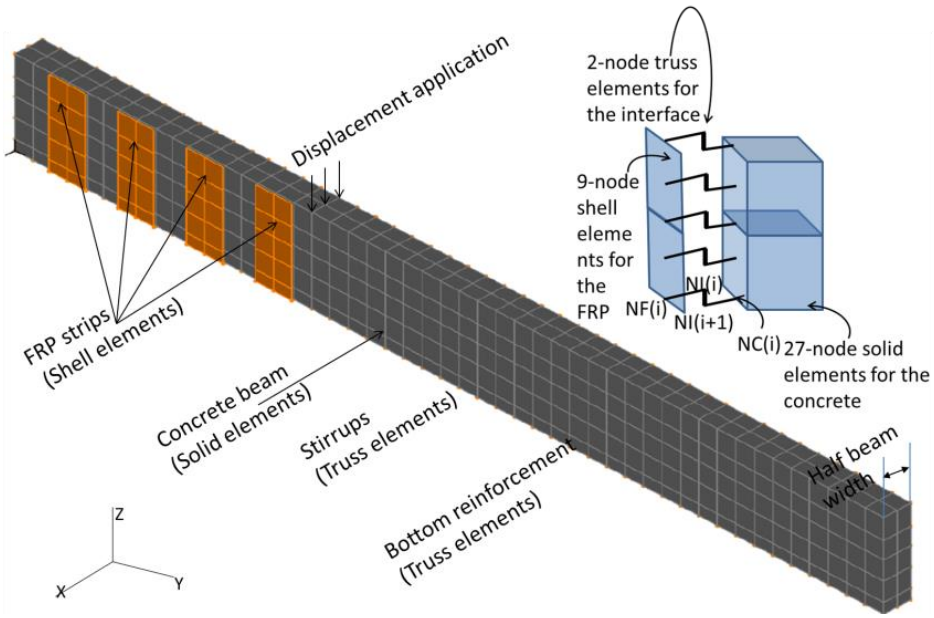


Figure 2. Finite element model for a strengthened specimen.

## 3 NUMERICAL RESULTS AND DISCUSSIONS

### *3.1 Ultimate load capacities, deflection profiles and modes of failure*

The experimental results of 12 specimens have been used to validate the finite element models that have accurately predicted the ultimate load capacities for the simulated beams as shown in the comparisons in Table 1. The predictions ranged between 96% and 111% with an average of 104% and a standard deviation of 4.0%, which indicates a very good agreement between the numerical and the experimental load capacities, $P_{u,num.}$, and $P_{u,exp.}$, respectively. It is shown from Figure 3 that the model accurately predicted the load–deflection curves for this specimen.

Table 1. Characteristics of specimens and experimental results.

| Designation | Description* | | | | | | $P_u$, exp. kN | $P_u$, num. mm | $P_u$, num. /$P_u$, exp. |
|---|---|---|---|---|---|---|---|---|---|
| | Strips | | | | Stirrups | Scheme | | | |
| | s, mm | w, mm | No. | Orien. | | | | | |
| R | NA | | | | No | | 66 | 67 | 1.02 |
| R-S | NA | | | | Yes | | 79 | 85 | 1.08 |
| M-4W-V | 190 | 100 | 4 | Vertical | No | M | 82 | 86 | 1.06 |
| M-4W-V-S | 190 | 100 | 4 | Vertical | Yes | M | 105 | 110 | 1.05 |
| B-6N-V | 125 | 50 | 6 | Vertical | No | B | 105 | 116 | 1.11 |
| B-6N-V-S | 125 | 50 | 6 | Vertical | Yes | B | 123 | 130 | 1.06 |
| BM-8N-V | 90 | 50 | 8 | Vertical | No | BM | 138 | 143 | 1.03 |
| BM-8N-V-S | 90 | 50 | 8 | Vertical | Yes | BM | 142 | 146 | 1.03 |
| BM-8N-I | 90 | 50 | 8 | Inclined | No | BM | 141 | 147 | 1.04 |
| BM-8N-I-S | 90 | 50 | 8 | Inclined | Yes | BM | 148 | 152 | 1.03 |
| BM-6N-V | 125 | 50 | 6 | Vertical | No | BM | 125 | 120 | 0.96 |
| BM-6N-V-S | 125 | 50 | 6 | Vertical | Yes | BM | 135 | 136 | 1.01 |

* s for spacing, w for width, no. for number of strips, orien. for strip orientation

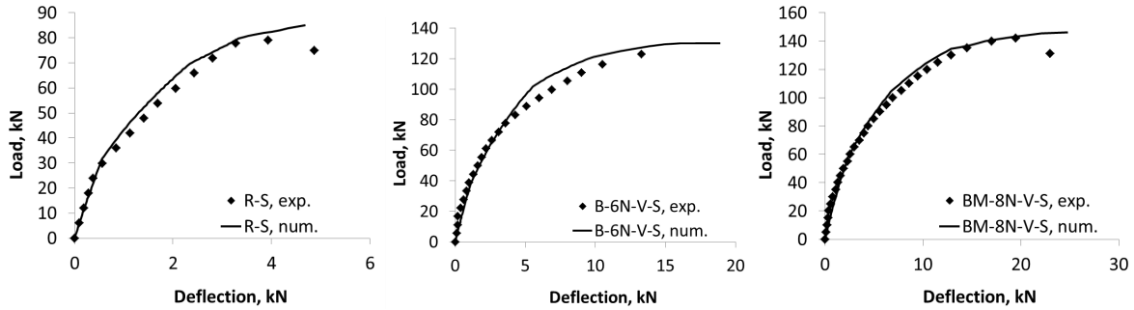


Figure 3. load deflection comparison for a reference specimen, EB and hybrid EB/MF specimen.

### *3.2 FRP/concrete interfacial behaviour*

The graphs in Figures 4a and 4b show samples of the interfacial shear slip profiles at failure for the EB and hybrid EB/MF specimens, respectively. The focus here is on the effect of using the fasteners along the bonded FRP strips on the interfacial shear stress distribution. It is useful to compare Figure 4a (for the EB specimen) with Figure 4b (for the hybrid EB/MF counterpart) in terms of the interfacial stress distribution. This is to assess the effect of the fasteners on the interfacial shear stress distribution within the bonded locations. Hybrid EB/MF specimens consistently show lower interfacial shear stresses at the ultimate load than those for the associated EB specimens. This is in fact an indication that the fasteners in the EB/MF specimens decreased possibilities of debonding by acting as locations of anchorage.

### *3.3 FRP-transverse steel interaction*

The main focus of this research paper is to study the interaction obetween the FRP strips and the transverse steel reinforcement. Figure 5 shows the effect of utilizing transverse steel reinforcement on the ultimate load capacities by showing the load increases due to the FRP/transverse steel reinforcement interaction for the different strengthening systems. In this figure the experimental results are used to examine such an interaction. The numerical finding

are in accord with the experimental counterpart as aformentioned indicated by the close prediction of the ultimate load carrying capacity of the finite element models. A reference comparison is first made between Specimens R–S and R with and without transverse steel reinforcement, respectively. The load capacity of Specimen R–S was found to be 20% higher than that of Specimen R that outpaced Specimen R–S to failure by 13 kN as shown in Figure 5. This is the experimentally-driven value for the contribution of the transverse steel reinforcement. As shown in Figure 5, the increase in the ultimate capacity of Specimen B-6N-V-S over the corresponding reference Specimen, R–S, is 41 kN. This increase represents the combined effect of the externally bonded FRP strips and the transverse steel reinforcement. As for Specimen B-6N-V, the increase in the ultimate load capacity over the corresponding reference specimen, R, is 39 kN. This indeed suggests that the transverse steel reinforcement has not been fully utilized as a result of the premature FRP debonding failure occurred as discussed earlier in the paper. It can also be seen that the effect of the transverse steel reinforcement is reduced with an increase in the effect of the EB strengthening represented by the gain in the load capacity.

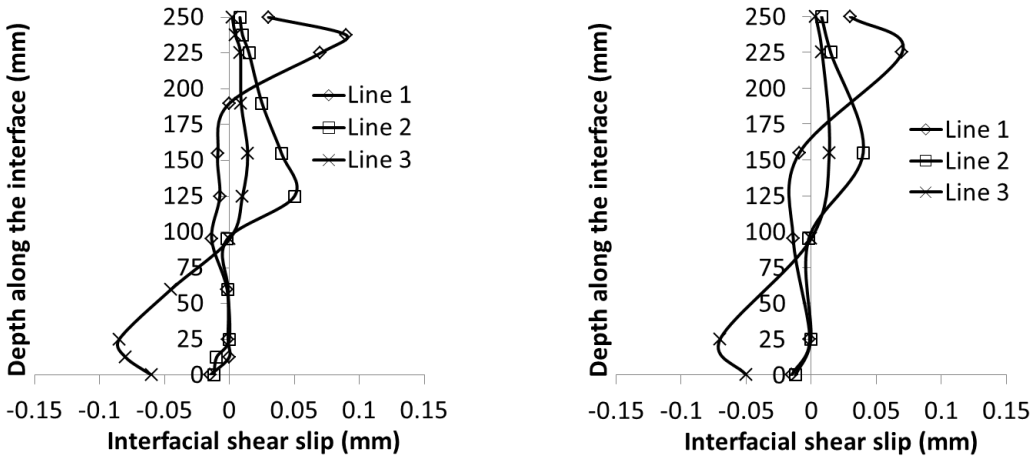


Figure 4. Interfacial shear stress-slip for externally bonded and hybrid strengthened specimens.

The mechanically fastened system; however, showed better efficacy of the transverse steel reinforcement by virtue of the elastopseudo-plastic nature of the bearing failure at the location of fasteners causing ductility of the strengthening system and therefore allowing the transverse steel reinforcement to be better utilized. This analysis is evident when comparing between the MF Specimens M-4W-V-S (with transverse steel reinforcement) and M-4W-V (without). The difference in the increases in the ultimate load carrying capacities of the two aforementioned specimens as in Figure 5 is 26–16 = 10 kN. Bearing in mind that the difference between the load capacities of Specimens R–S and R is 13 kN, one may conclude that the ductile nature of the mechanically fastened system allows better interaction between the external strips and the internal transverse steel reinforcement when compared to the externally bonded system. However, the FRP/concrete interaction is attained only at the location of fasteners.

For the hybrid EB/MF Specimen BM-6N-V-S, the increasein the ultimate capacity is 2 kN greater than that of Specimen BM-6N-V. Here the specimens actually did not fail in shear but rather failed due to FRP detachment combined with tension steel yielding. Therefore, the actual

FRP/transverse steel reinforcement interaction cannot be evaluated. Similar observation applies for Specimens BM-8N-V-S and BM-8N-I-S when compared to Specimens BM-8N-V and BM-8N-I, respectively. The differences in the load carrying capacities between Specimens BM-8N-V-S and BM-8N-I-S, on the one hand, and Specimens BM-8N-V and BM-8N-I, on the other hand were 7 and 4 kN, respectively, in favor of the former specimens of which average is less than that between the reference specimens. As experimentally indicated (Ebead and Saeed 2013), the crack inclination changes as a result of strengthening. Therefore, the contribution of the transverse steel reinforcement will decrease as a result of such an inclination of the shear crack that intersects less with the transverse reinforcement.

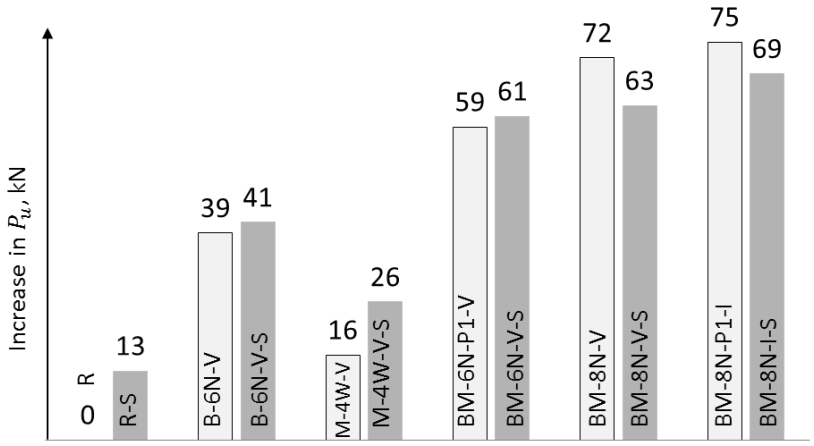


Figure 5. Load increases for specimens with and without transverse steel reinforcement, kN.

## 4 CONCLUSIONS

Finite element models for RC beams shear strengthened using FRP composites were created in this study. Available experimental results were used to verify the models. The strengthened specimens were classified according to the strengthening scheme as MF and hybrid EB/MF-FRP strengthened specimens. The concrete microplane model was used as a user-defined subroutine in the finite element package. Moreover, discrete interface elements were used at the bonded and the mechanically fastened locations. These elements accommodated the vertical and inclined FRP strips using appropriate constraint equations. The predictions of the ultimate load capacities were fairly accurate when compared to the available experimental results. The average numerical to experimental ultimate load ratio is 1.04 with a standard deviation of 4%. This indicates the prediction quality of the model in estimating the load capacity with reasonable accuracy.

Interfacial shear stress–slip and interfacial bearing stress–slip models were successfully used to define the constitutive behaviour of the discrete interface elements to properly simulate the FRP/concrete interfacial behaviour. The main conclusions out of the comparisons among the interfacial behaviour for the different simulated beams are that: (1) fasteners provided anchorage along the bonded length that led to a profound improvement of the bond behaviour; and (2) the ductile nature of the MF-FRP system allowed for high interfacial slips for the strengthened specimen with this system as compared to those strengthened using the EB and the hybrid EB/MF counterparts. This indicates an effective utilization of the MF system for beam shear strengthening. The FRP/stirrups has also been discussed and it was indicated that different responses have been experienced for the three strengthenig systems.

## 5 ACKNOWLEDGEMENT

This paper was made possible by NPRP grant # NPRP 7-1720-2-641 from the Qatar National Research Fund (a member of Qatar Foundation). The statements made herein are solely the responsibility of the author.

## 6 REFERENCES

Abdel Baky, H., U. A. Ebead and K. W. Neale (2007). "Flexural and interfacial behavior of FRP-strengthened reinforced concrete beams." *Journal of Composites for Construction*, 11(6): 629-639.

Bank, L. C. and D. Arora (2007). "Analysis of RC beams strengthened with mechanically fastened FRP (MF-FRP) strips." *Composite Structures*, 79(2): 180-191.

Bathe, K. J. (2005). ADINA. Watertown, MA, USA, ADINA R & D, Inc.

Bažant, Z., F. Caner, I. Carol, M. Adley and S. Akers (2000). "Microplane model M4 for concrete. I: Formulation with work-conjugate deviatoric stress." *Journal of Engineering Mechanics*, 126(9): 944-953.

Caner, F. and Z. Bažant (2000). "Microplane model M4 for concrete. II: Algorithm and calibration." *Journal of Engineering Mechanics*, 126(9): 954-961.

Chen, G. M., J. F. Chen and J. G. Teng (2012). "On the finite element modelling of RC beams shear-strengthened with FRP." *Construction and Building Materials*, 32: 13-26.

Ebead, U. and H. Marzouk (2005). "Tension-stiffening model for FRP-strengthened RC concrete two-way slabs." *Materials and structures*, 38(2): 193-200.

Ebead, U. and H. Saeed (2014). "Numerical Modeling of Shear Strengthened Reinforced Concrete Beams Using Different Systems." *Journal of Composites for Construction*, 18(1): 04013031.

Ebead, U. A. (2011). "Hybrid externally bonded/mechanically fastened fiber-reinforced polymer for RC beam strengthening." *ACI Structural Journal*, 108(6): 669-678.

Ebead, U. A. and H. Saeed (2013). "Hybrid shear strengthening system for reinforced concrete beams: An experimental study." *Engineering Structures*, 49: 421-433.

Ebead, U. A. and H. A. Saeed (2010). "Modeling of reinforced concrete slabs strengthened with fiber-reinforced polymer or steel plates." *ACI Structural Journal*, 107(2): 218-227.

Elsayed, W., U. A. Ebead and K. W. Neale (2007). "Interfacial behavior and debonding failures in FRP-strengthened concrete slabs." *Journal of Composites for Construction*, 11(6): 619-628.

Elsayed, W. E., U. A. Ebead and K. W. Neale (2009). "Mechanically fastened FRP-strengthened two-way concrete slabs with and without cutouts." *Journal of Composites for Construction*, 13(3): 198-207.

Elsayed, W. E., U. A. Ebead and K. W. Neale (2009). "Studies on mechanically fastened fiber-reinforced polymer strengthening systems." ACI Structural Journal 106(1): 49-59.

Godat, A., P. Labossiere and K. W. Neale (2012). "Numerical investigation of the parameters influencing the behaviour of FRP shear-strengthened beams." *Construction and Building Materials*, 32(7): 90-98.

Godat, A., P. Labossière, K. W. Neale and O. Chaallal (2012). "Behavior of RC members strengthened in shear with EB FRP: Assessment of models and FE simulation approaches." *Computers & Structures* 92–93(2): 269-282.

Godat, A., K. W. Neale and P. Labossière (2007). "Numerical modeling of FRP shear-strengthened reinforced concrete beams." *Journal of Composites for Construction*, 11(6): 640-649.

Kotynia, R., H. Abdel Baky, K. W. Neale and U. Ebead (2008). "Flexural strengthening of RC beams with externally bonded CFRP Systems: Test results and 3D nonlinear FE analysis." *Journal of Composites for Construction* 12(2): 190-201.

Lamanna, A. J., L. C. Bank and D. T. Borowicz (2004). "Mechanically fastened FRP strengthening of large scale RC bridge T beams." *Advances in Structural Engineering*, 7(6): 525-538.

Lamanna, A. J., L. C. Bank and D. W. Scott (2004). "Flexural strengthening of reinforced concrete beams by mechanically attaching fiber-reinforced polymer strips." *Journal of Composites for Construction*, 8(3): 203-210.

Neale, K. W., U. A. Ebead, H. Abdel Baky, W. E. Elsayed and A. Godat (2006). "Analysis of the load-deformation behaviour and debonding for FRP-strengthened concrete structures." *Advances in Structural Engineering*, 9(6): 751-763.